

Variable low-temperature scanning tunneling microscopy study of Si(001): Nature of the $2\times 1 \rightarrow c(2\times 4)$ phase transition

A. R. Smith, F. K. Men, K.-J. Chao, and C. K. Shih
University of Texas at Austin, Austin, Texas 78712

(Received 25 July 1995; accepted 22 November 1995)

We have studied the Si(001) surface from 120 K to room temperature using a variable low-temperature scanning tunneling microscope. Complementary investigations were carried out on two distinctly different types of surfaces: first, the normal 2×1 surface and second, the $2\times n$ ($4 < n < 12$) surface. For the 2×1 surface, the defects are scattered randomly. By plotting out the fraction of buckled dimers as a function of temperature, we find a slow transition from predominantly $c(2\times 4)$ at low temperature to mostly 2×1 at room temperature for a defect concentration of about 8.5%. For the $2\times n$ surface, the much larger number of surface vacancies form long-range ordered chains, dividing the surface into many short dimer segments. These dimer segments predominantly appear to be unbuckled at room temperature. Upon cooling to 190 K, we observe very little change in the amount of buckling. The implications of this result are discussed.

© 1996 American Vacuum Society.

I. INTRODUCTION

Although it has been known for a long time that the Si(001) surface exhibits a 2×1 reconstruction at (RT),¹ controversy has surrounded the topic of the exact nature of the dimers. Theoretical studies have lent support to two different models of the surface dimers, namely, the symmetric and asymmetric dimer models.²⁻⁶

Experimental investigations have also attempted to verify one or the other model. Scanning tunneling microscopy (STM) images have shown symmetric-appearing dimers at RT except in the vicinity of defects and step edges where buckled dimers are observed.^{7,8} A variable temperature low-energy electron diffraction (LEED) investigation has shown, however, that the surface undergoes a reversible phase transition at around 200 K.⁹ The first low-temperature (LT) STM images of this surface showed that at LTs the surface is indeed largely composed of buckled dimers.¹⁰ However, those images showed that a fair fraction of symmetric-appearing dimers remain.

Additionally, most of the buckled dimers were arranged into the $c(2\times 4)$ structure although regions of $p(2\times 2)$ also coexisted. This was attributed to the defect density on the surface (about 5%–10% in that work). A number of more recent works have aimed to obtain a low defect concentration and, by so doing, remove their influence.^{11,12}

In the present study, rather than jump into the controversy of whether dimers are intrinsically symmetric or asymmetric, we choose to focus on the following questions. First, what is the nature of the phase transition, and second, what is the role played by defects in the phase transition? Several recent theoretical works have aimed at addressing this issue.^{13,14} We consider that there are two possibilities, namely that it is either a first order or a second order (also referred to as continuous) phase transition. If it is actually first order, then, through careful experimentation, we should be able to observe the nucleation and growth of reconstructed [i.e., $c(2\times 4)$] domains near the transition temperature. On the other

hand, if it really is a second order phase transition, then, by mapping out the order parameter, i.e., the percentage of buckled dimers, as a function of temperature, we should be able to deduce the critical exponent. Either result should prove interesting.

A complete understanding of this phase transition should explain why the surface at low temperature exhibits primarily $c(2\times 4)$ rather than $p(2\times 2)$ symmetry. This question may also be related to the surface defects. A recent STM result has concluded that certain “C-type” defects act as phase shifters with regard to the buckling pattern, thus inducing local regions of $p(2\times 2)$ on an otherwise perfect $c(2\times 4)$ reconstruction.¹¹ However, the question remains as to why the surface seems to prefer the $c(2\times 4)$ arrangement and how it gets into that state.

The LEED study mentioned above found that the phase transition took place over a fairly broad temperature range.⁹ Thus, the authors concluded that this is a second order order–disorder transition. However, their result lacked a quantification of the defect type and concentration on the surface. A theoretical article has predicted that as little as 1% defect concentration could reduce the order parameter by 75%, resulting in a smearing out of the transition over a fairly broad temperature range.¹³ Based on this prediction, it would then appear that since the best Si(001) surfaces reported thus far have around $\frac{1}{2}\%$ –1% defects, it may not be possible to ever entirely remove their influence on the phase transition. Thus the difficulty remains for identifying the true nature of the phase transition.

The key to making progress on these issues appears to be to gain a more complete quantitative as well as qualitative understanding of how the different types of surface defects influence the phase transition. To that end, we have performed a comparative investigation between normal 2×1 surfaces having defect concentrations of about 8.5% and $2\times n$ surfaces where the defects are almost all vacancies which form long-range ordered chains running normal to the

dimer row direction. Since the symmetric vacancies do not appear to induce buckling in the case of the normal 2×1 surfaces, it is interesting to ask the question what will happen to this surface at low temperature. If, for example, the short dimer segments do not buckle, then this may shed some light on the issue of dimer buckling itself.

II. EXPERIMENT

It is clear then that in order to carry out this investigation, the tool of choice should be able to measure both the fraction of buckled dimers as a function of temperature as well as to quantify both the number and type of surface defects. Thus it would appear that a variable low-temperature STM would be the tool of choice for this investigation. Our experiments are carried out in an ultrahigh vacuum (UHV) chamber specifically designed for use with our home-built variable low-temperature STM.¹⁵ The chamber is also equipped with LEED and various sample and tip preparation facilities. Samples and tips can both be transferred into the main chamber through a load lock. Typical pressure in the main chamber is 6×10^{-11} Torr.

Tips are prepared using electrochemical etching of polycrystalline W wires. They are treated prior to use inside the chamber with electron bombardment. Samples used are from either 0.08° or 0.5° miscut (001)-oriented wafers made by Wacker Chemitronic Corp. Most of the work used the lower miscut samples. Low defect surfaces are usually prepared in the standard way: outgassing for a period of time at 700°C , followed by a quick flash to about 1200°C , followed by a slow anneal starting at about 950°C . In one case, we first did an *ex situ* chemical treatment before heating the crystal inside the chamber. The $2\times n$ surfaces are prepared in a similar way except that, rather than anneal the sample, the temperature is quenched from 1200°C to RT. Repeated quenching cycles finally result in a $2\times n$ or partial $2\times n$ structure.

III. 2×1 SURFACES

In Fig. 1(a), we show an image of a normal Si(001) surface at room temperature acquired at a sample bias of -2.84 V and a tunneling current of 0.65 nA. This surface is composed of Si dimers, various combinations of symmetric-appearing missing dimer defects, and other asymmetric-appearing defects, which have also been discussed in prior work.^{7,8,10-12} The total defect concentration for this image is about 13.5%. This leads to a fairly high percentage of buckled dimers. At this temperature, the buckling appears to begin at the asymmetrical-shaped defects, as also pointed out previously.¹⁰⁻¹² The buckling propagates for a short distance (6–8 dimers) and dies out. Close inspection reveals that the buckling does not start at single missing dimer defects, double missing dimer defects, or combinations of these. However, such defects may serve to interrupt the buckling pattern or terminate it at that point. It is also evident that large domains of $c(2\times 4)$ are not observed at room temperature even for high defect concentrations, but rather there exist fairly large domains of symmetric appearing dimers, as seen towards the center of the image.

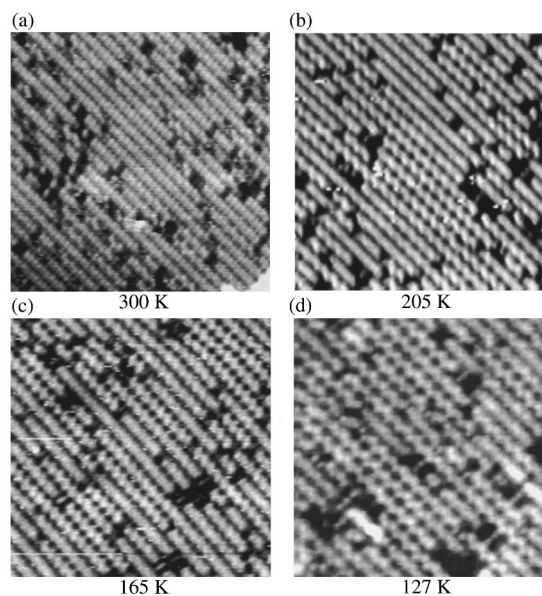


FIG. 1. (a) A $174\text{ \AA}\times 174\text{ \AA}$ room-temperature STM image of a fairly high defect (13.5%) Si(001) surface recorded at -2.84 V sample bias and 0.65 nA tunneling current. Buckling appears to be localized near the defects. (b) Surface with slightly less defect density (10%) imaged at -2.69 V sample bias and 0.39 nA tunneling current at 205 K. Extended regions of buckled dimers are apparent; most regions have the $c(2\times 4)$ structure. (c) At 165 K, about 85% of the dimers are at least partly buckled. (d) At 127 K the surface is over 95% buckled, with $c(2\times 4)$ making up 59% and $p(2\times 2)$ 24% of the total.

In contrast to the room T surface, we observe in Fig. 1(b) that the Si(001) surface at 205 K, namely near the transition temperature, is composed of an increased concentration of buckled dimers. This image contains about 10% defects. Here, we observe that the dimer buckling within a given row appears to propagate further along the row as compared to the room-temperature surface. A close inspection of the image reveals that where two rows of buckled dimers lie adjacent to one another, they are usually in the $c(2\times 4)$ arrangement, although an appreciable $p(2\times 2)$ fraction also exists.

At 165 K, the fraction of buckled dimers on the surface is even larger, as seen in the image of Fig. 1(c). Here we find very few places on the surface where there exist more than two adjacent dimer rows having only symmetric-appearing dimers. At even lower temperature, namely at 127 K as shown in Fig. 1(d), the surface is mostly composed of buckled dimers.

The preceding gives the general picture for the behavior of this surface as a function of temperature. With a sufficient database, however, it is possible to do a more thorough data analysis. Though somewhat painstaking, our method of analysis is the following: we begin by simply counting the number of buckled dimers to determine the buckling fraction at different temperatures. In many cases, however, even with a high quality image it is difficult to judge the amount of buckling without introducing inconsistency from image to image. In fact, this is not just an issue of image quality since a whole range of buckling exists, from weakly buckled to

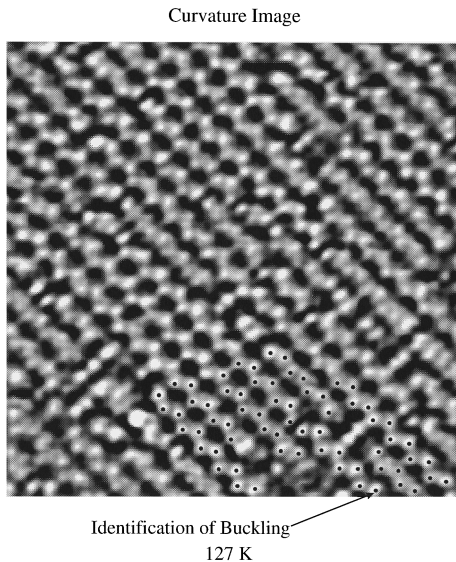


FIG. 2. Curvature image corresponding to the image shown in Fig. 1(d) at 127 K. The buckling is enhanced, aiding in the identification of the buckled dimers. Black dots exemplify the marking process used in the data analysis.

strongly buckled. In principle, one should be able to define a buckling amplitude.

To simplify matters, we choose to count every dimer that appears at all buckled. In order to do so, we employ the curvature image that can easily be calculated from the raw data. Such a curvature image is shown in Fig. 2 and corresponds to Fig. 1, which was taken at 127 K. As can be seen, the curvature image amplifies the buckling such that slight buckling can be more clearly identified. After the curvature image is produced, all of the apparently buckled dimers are marked and counted. At the bottom part of the image of Fig. 2 is shown a sample of the marking of the buckled dimers which is done for each image in the analysis. Additionally, we count the total number of defects within the image which then gives us the defect concentration. Subtracting the total number of defects from the total number of dimer sites, as computed from the total area of the image, gives us the total number of dimers on the surface. Dividing the number of buckled dimers by the total number of dimers yields the buckled dimer fraction for that image and at that temperature. Doing the same for images at many different temperatures then allows us to plot out the fraction of buckled dimers along with the defect concentration as a function of temperature.

We have carried out such an analysis from our data set, and the results are shown in Fig. 3(a) together with the corresponding defect concentrations. Note that all of the points are from the same sample except for the point at 246 K, which we add for reference to compare with the rest of the data. Here, most points represent up to several thousand dimers. Despite the remaining fluctuations, it is clear that as the temperature is reduced, the percentage of buckling increases gradually over a certain range near the expected transition temperature, in agreement with Murata's LEED result.⁹ Notice also that the defect concentration fluctuates

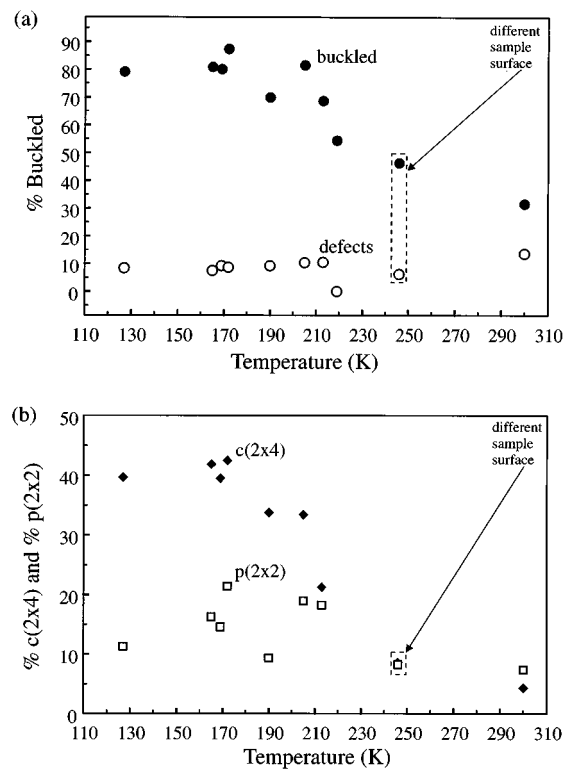


FIG. 3. (a) Graph of the percentage of buckled dimers as a function of temperature. Filled circles indicate the buckling; empty circles indicate the defect concentration. Some of the points represent over three thousand dimers. The average defect concentration is about 8.5% but fluctuates between 6.5% and 13.5%. (b) Graph of the separate percentages of $c(2 \times 4)$ (diamond-shaped symbols) and $p(2 \times 2)$ (open squares) as a function of temperature. The $c(2 \times 4)$ increases with decreasing temperature while the $p(2 \times 2)$ fluctuates.

from image to image, averaging around 8.5%.

We can get more information out of the images by counting the fraction of buckled dimers that are in the $c(2 \times 4)$ arrangement and the fraction that are in the $p(2 \times 2)$ arrangement. The method is to compare each buckled dimer in a given row with the dimer in the row next to it, for example, to the left. If they are buckling in opposite directions, then that is one $c(2 \times 4)$ unit; if they are buckling in the same direction, then that is one $p(2 \times 2)$ unit. This is repeated for every buckled dimer within every row of the image. Summing all the $c(2 \times 4)$ and $p(2 \times 2)$ units and dividing each sum by the total number of dimers, we finally arrive at the percentages of $c(2 \times 4)$ and $p(2 \times 2)$. For the image shown in Fig. 1(c), for example, the fraction of $c(2 \times 4)$ is 45%; for $p(2 \times 2)$ it is 20%. Notice that these two percentages do not add up to the total percentage of buckled dimers (85%) since this does not include the isolated buckled chains.

In Fig. 3(b) are shown the results of this counting analysis, based on the same data sets as those used for the plots of Fig. 3. Clearly, the percentage of $c(2 \times 4)$ increases as the temperature decreases over a certain range around the expected transition temperature while the percentage of $p(2 \times 2)$ fluctuates without a strong trend. If $p(2 \times 2)$ regions are really related to the defects, then one may expect that as the

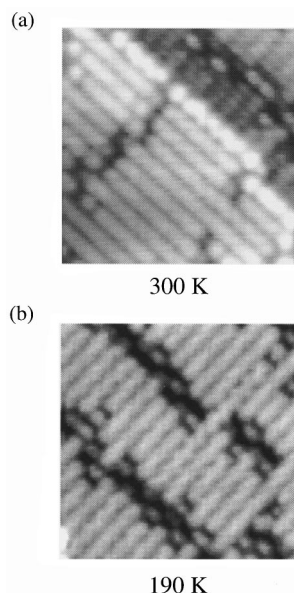


FIG. 4. (a) A $100 \text{ \AA} \times 100 \text{ \AA}$ room-temperature image of a partial $2 \times n$ surface with defect chains running perpendicular to the dimer rows. Image was acquired at -2.74 V sample bias and 0.52 nA tunneling current. Almost no buckling is observed, except at the step edge. (b) Partial $2 \times n$ surface at 190 K acquired under similar biasing conditions. Buckling is confined to the longer dimer segment crossing over the defect chain.

defect concentration is reduced, the amount of $p(2 \times 2)$ will also reduce for all temperatures. Further work will be needed to verify this point.

IV. $2 \times n$ SURFACES

For comparison with the low defect surfaces, we also investigated the temperature dependence of the $2 \times n$ surface. Such a surface has chains of defects running in a direction perpendicular to the dimer row direction. Thus the surface is divided into short dimer segments. Shown in Fig. 4(a) is a room-temperature image of such a surface. All the dimers within this image appear to be unbuckled, except for those on the step edge. A detailed room-temperature study of this surface was carried out, detailing the nature of this structure, and will not be repeated here.¹⁶ Shown in Fig. 4(b) is a typical image of the $2 \times n$ surface at 190 K , just below the expected transition temperature. Interestingly enough, dimer buckling is still rarely seen, except in isolated locations such as where a dimer segment bridges across the defect chain.

It has been suggested by Neddermeyer *et al.* that dimers on Si(001) are intrinsically buckled, independent of temperature but oscillating at RT. Near type-C defects, the dimers are only prevented from oscillating, giving rise to the buckled appearance. At LT, the buckling is related to the freezing out of the thermally induced oscillation. If this viewpoint is correct, then how does one explain the lack of observation of

buckled dimers at 190 K on the $2 \times n$ surface? Does this mean that dimers on the $2 \times n$ surface for some reason will not stop oscillating at LT? A possibility is that 190 K is still not low enough to freeze out the thermal motion of the dimers, but they may actually freeze out at some lower temperature. Further experiments will be necessary to verify this point. On the other hand, for a longer dimer row we do observe buckling at 190 K . These observations should have implications for the underlying mechanism of dimer buckling.

V. SUMMARY

We carried out a study of 2×1 and $2 \times n$ surfaces of Si(001) as a function of temperature. The 2×1 surface shows buckling at all temperatures with the amount of buckling increasing at lower temperatures, similar to observations reported previously by others. We have found that the percentage of $c(2 \times 4)$ does increase as temperature decreases while the percentage of $p(2 \times 2)$ appears to fluctuate. However, in order to address the nature of the phase transition, we need to perform the same temperature-dependent study over a range of different defect concentrations. The lack of observation of buckling at LT on the $2 \times n$ surface calls for a new understanding of the buckling mechanism itself.

ACKNOWLEDGMENTS

This work was partly supported by the National Science Foundation (Grant No. DMR-94-02938), a Texas Instruments University Research Grant, and the Science and Technology Center Program of the National Science Foundation (Grant No. CHE8920120).

- ¹R. E. Schlier and H. E. Farnsworth, *J. Chem. Phys.* **30**, 917 (1959).
- ²D. J. Chadi, *Phys. Rev. Lett.* **43**, 43 (1979).
- ³J. Ihm, M. L. Cohen, and D. J. Chadi, *Phys. Rev. B* **21**, 4592 (1980).
- ⁴K. C. Pandey, in *Proceedings of the 17th ICPS*, edited by D. J. Chadi and W. A. Harrison (Springer, Berlin, 1984), p. 55.
- ⁵M. C. Payne, N. Roberts, R. J. Needs, M. Needels, and J. D. Joannopoulos, *Surf. Sci.* **211/212**, 1 (1989).
- ⁶J. Dabrowski and M. Scheffler, *Appl. Surf. Sci.* **56–58**, 15 (1992).
- ⁷R. J. Hamers, R. M. Tromp, and J. E. Demuth, *Phys. Rev. B* **34**, 5343 (1986).
- ⁸R. M. Tromp, R. J. Hamers, and J. E. Demuth, *Phys. Rev. Lett.* **55**, 1303 (1985).
- ⁹T. Tabata, T. Aruga, and Y. Murata, *Surf. Sci. Lett.* **179**, L63 (1987).
- ¹⁰R. A. Wolkow, *Phys. Rev. Lett.* **68**, 2636 (1992).
- ¹¹H. Tochiohara, T. Amakusa, and M. Iwatsuki, *Phys. Rev. B* **50**, 12262 (1994).
- ¹²D. Badt, H. Wengelnik, and H. Neddermeyer, *J. Vac. Sci. Technol B* **12**, 2015 (1994).
- ¹³K. Inoue, Y. Morikawa, K. Terakura, and M. Nakayama, *Phys. Rev. B* **49**, 14774 (1994).
- ¹⁴D. K. Stillinger and F. H. Stillinger, *Phys. Rev. B* **48**, 15047 (1993).
- ¹⁵A. R. Smith and C. K. Shih, *Rev. Sci. Instrum.* **66**, 2499 (1995).
- ¹⁶F. K. Men, A. R. Smith, K.-J. Chao, and C. K. Shih, *Phys. Rev. B* **52**, R8650 (1995).